JOURNAL OF Materials CHEMISTRY

The first hexagonal columnar discotic liquid crystalline carbazole derivatives induced by noncovalent π–π interactions†‡

M. Manickam,[a] Maura Belloni,[a] Sandeep Kumar,[b] Sanjay K. Varshney,[b] D. S. Shankar Rao,[b] Peter R. Ashton,[a] Jon A. Preece*[a] and Neil Spencer[a]

[a]*School of Chemistry, University of Birmingham, Edgbaston, Birmingham, UK B15 2TT. E-mail: j.a.preece@bham.ac.uk*
[b]*Centre for Liquid Crystal Research, P.O. Box 1329, Jalahalli Bangalore–560 013, India*

Received 4th April 2001, Accepted 22nd June 2001
First published as an Advance Article on the web 1st October 2001

The synthesis of 13 discotic mesogens is described in which the well-known hexakis(pentyloxy)triphenylene liquid crystalline material has been chemically modified to incorporate one, two, three and six carbazole moieties. These modifications have been achieved by the alkylation or esterification of mono-, di-, tri- and hexa-hydroxytriphenylene derivatives with alkyl bromides and carboxylic acids incorporating the carbazole moiety. The pure compounds are not liquid crystalline in nature but when doped with TNF, hexagonal columnar mesophases are induced, as shown by DSC, OPM and X-ray diffraction. These mesophases exist below room temperature. The mesophase clearing temperatures are dependent on several factors including the chain length separating the carbazole moiety from the triphenylene core, and the nature of the ether or ester linkage, and the degree of TNF doping. The data suggest that the most stable mesophases (highest clearing temperatures) are formed when a 2 : 1 complex is formed between the carbazole derivatives and the TNF, respectively. The correlation length obtained from X-ray diffraction reveals that the columnar order for one of the ether derivatives decreases, whereas the correlation length increases for one of the ester derivatives. This result suggests that the TNF is not only partaking in π–π noncovalent bonding interactions, but also in polar interactions with the C=O bond. Such mesogenic carbazole derivatives may have advantageous photorefractive properties over the amorphous polymeric materials.

1. Introduction

Due to their extensive biological activity carbazole derivatives and their chemistry have been studied at length.[1] However, it is only recently that they have been studied in terms of their material properties[1,2] and in particular their photorefractive properties.[3] The interest in photorefractive materials[4] lies in their numerous potential technological applications,[5] such as high density optical data storage, optical image processing, phase conjugated mirrors, dynamic holography, optical computing, parallel optical logic, and pattern recognition. Thus, recent studies on carbazole materials have been concerned with electroluminescence,[6] nonlinear optics,[7] and photoconductivity.[8] Amorphous organic photorefractive materials[9] have many advantages over crystalline inorganic[3] and latterly crystalline organic[10] photorefactive materials on which the early research was carried out. These advantages include large optical nonlinearities, low relative permittivities, low cost, structural flexibilty, and ease of fabrication. However, the major drawback of the amorphous organic photorefractive materials is that a low T_g is required in order that the material can be aligned by a dc electric field to induce a degree of anisotropic ordering.[11] The chemical modification of the carbazole moiety to induce liquid crystallinity is attractive in order to combine the advantages of the amorphous materials with anisotropic ordering. However, to date there are only a few examples in which the carbazole moiety has been incorporated into thermotropic low molecular weight and polymeric liquid[12] crystalline materials and into lyotropic liquid crystals.[13] Furthermore, as far as we are aware, there are no examples of low molecular weight thermotropic hexagonal columnar discotic liquid crystals which incorporate the carbazole. Thus, one of the approaches that we are adopting[14] to induce hexagonal columnar discotic mesophases in carbazole derivatives is the covalent modification of the carbazole moiety with the well-known[15] discotic triphenylene derivatives. Here we report (i) the synthesis of several carbazole triphenylene hybrid structures in which one (**1a**–**e**), two (**2a**–**b**), three (**3a**–**b** and **4a**–**b**) and six (**5a**–**b**) carbazole units are covalently linked to the periphery of the triphenylene core and (ii) the induced mesophase behaviour of some of these carbazole derivatives when "complexed" with trinitrofluorenone (TNF).[16] The chemical structures of the carbazole derivatives are shown in Fig. 1.

2. Results and discussion

2.1 Synthesis

The synthesis (Scheme 1) of the mono-, bis- and tris-carbazole derivatives relies upon the mono-, bis- and tris-dealkylation of the parent hexakis(pentyloxy)triphenylene **6a** (R = C_5H_{11}) with bromocatecholborane[17] to afford the monohydroxy **7**, the dihydroxy **8**, the C_3 symmetrical trihydroxy derivative **9** and the asymmetrical trihydroxy derivative **10**. The hexahydroxy derivative **11** is prepared by a full demethylation of hexamethoxytriphenylene **6b** (R = CH_3)[18] The hexakis(alkyloxy)triphenylenes **6a** and **6b** are synthesised *via* a trimerisation of the corresponding 1,2-dialkoxybenzene derivatives with $FeCl_3$.[19]

†Basis of a presentation given at Materials Discussion No. 4, 11–14 September 2001, Grasmere, UK.
‡Electronic supplementary information (ESI) available: tables of reagents and conditions for the synthesis of **1b**, **2a**, **3a**, **4a**, **5a**, **1d**, **1e**, **2b**, **3b**, **4b**, **12b**, **13a**, **13b** and **13c**. See http://www.rsc.org/suppdata/jm/b1/b103052n/

 DOI: 10.1039/b103052n

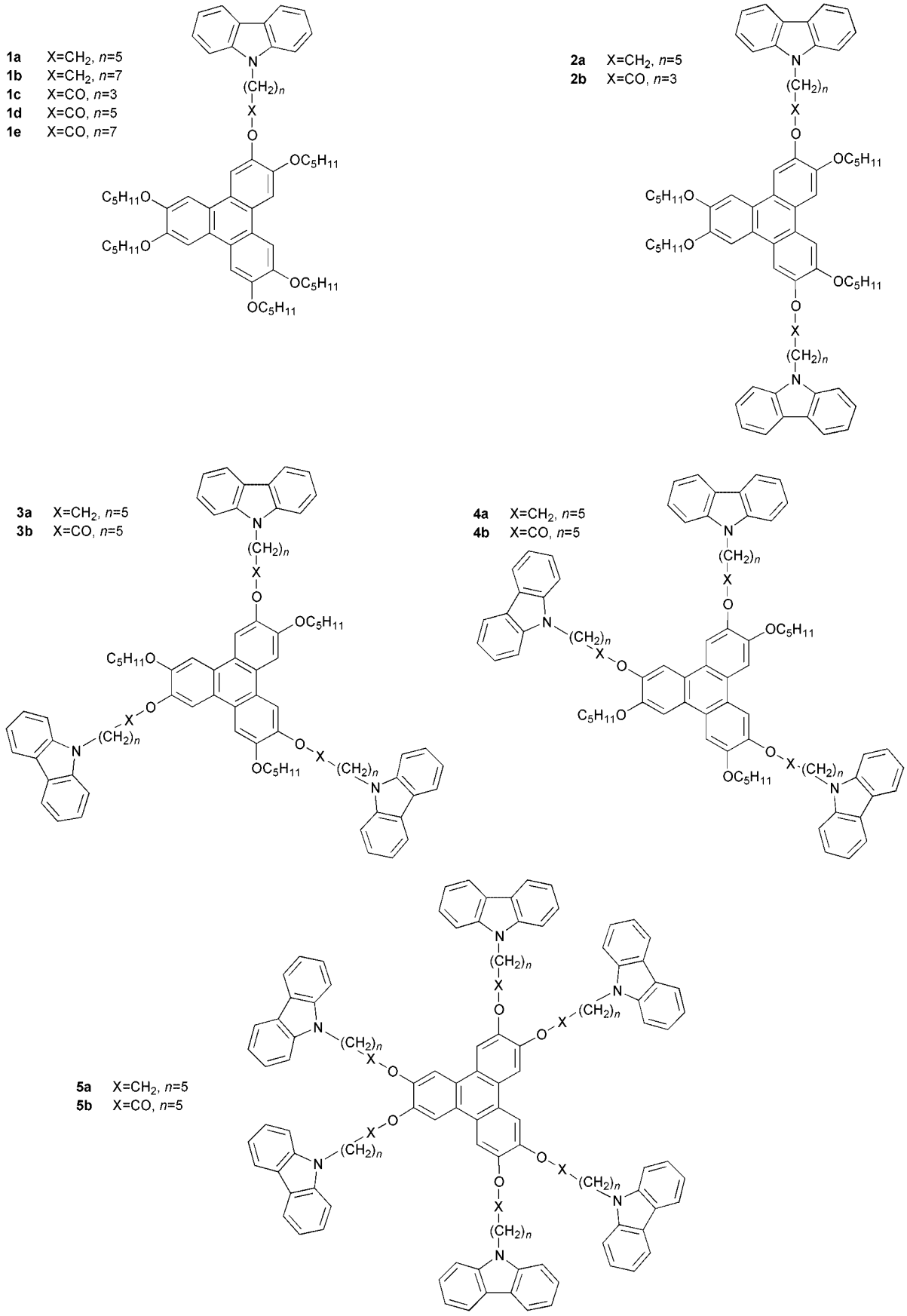

Fig. 1 Molecular structures of the carbazole derivatives studied in this paper.

The N-alkylation[20a] of carbazole with 1,6-dibromohexane or 1,8-dibromooctane affords the alkyl bromides **12a** and **12b** (Scheme 2) which are then carried forward in O-alkylation reactions of the hydroxytriphenylene derivatives **7**–**11** to afford the ether linked derivatives **1a**, **1b**, **2a**, **3a**, **4a** and **5a**. N-Alkylation[20b] of the carbazole with methyl 4-bromobutanoate, methyl 6-bromohexanoate, and methyl 8-bromooctanoate afforded the three esters **13a**–**c**. These esters were subsequently hydrolysed to the carboxylic acids **14a**–**c** (Scheme 2). The acids **14a**–**c** were then coupled to the hydroxytriphenylene

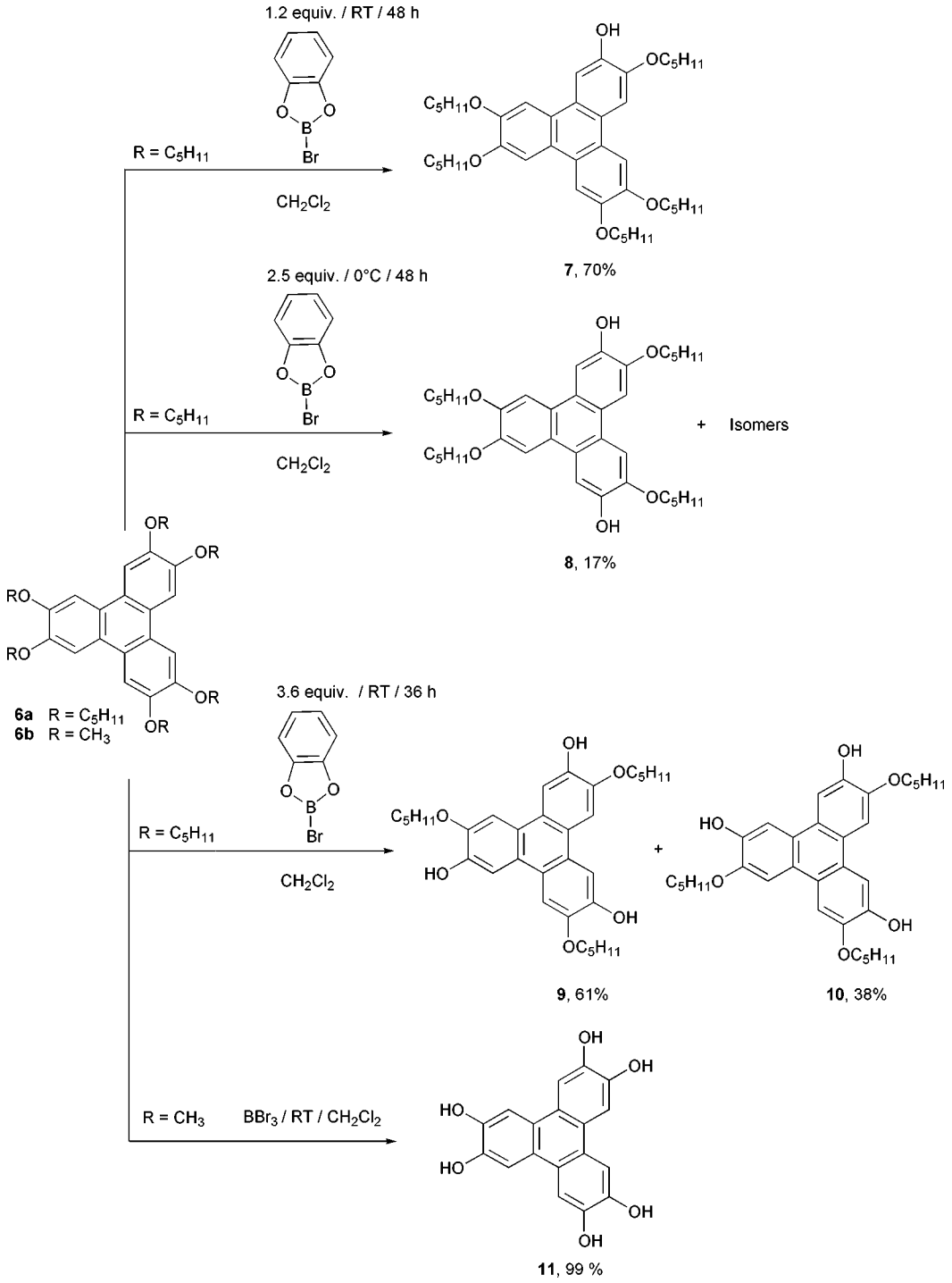

Scheme 1 Synthetic routes to the hydroxytriphenylene derivatives **7**–**11**.

derivatives **7**–**10** using DCC–DMAP to afford the ester linked carbazole derivatives **1c**, **1d**, **1e**, **2b**, **3b**, and **4b** (Scheme 3). The synthesis of **5b** required a slightly different route than was required for the less substituted esters, because of the poorer solubility of the hexahydroxy derivative **11**. Thus, **11** was coupled with the acid chloride **15b** (prepared from the acid **14b** and thionyl chloride). The synthesis of **12** was also accompanied by the isolation of **12a.dimer** as a minor by-product.

2.2 Phase behaviour of the carbazole derivatives as a function of temperature

The differential scanning calorimetric (DSC) analysis of compounds **1**–**4** revealed that none of the materials possessed liquid crystalline behaviour, and were either crystalline or amorphous materials which underwent various solid–solid phase changes as they were heated at 10 °C min^{-1} and finally yielding the isotropic liquid. Tables 1 and 2 (first entry) highlight the melting behaviour of the pure derivatives **1**–**5**.

Optical polarised microscopy (OPM) confirmed our observations from DSC and none of the materials were birefringent liquids.

2.3 Phase behaviour of binary mixtures of the carbazole derivatives and trinitrofluorenone as a function of temperature

Undeterred by the lack of liquid crystallinity displayed by the carbazole derivatives, we set about investigating whether it was possible to induce liquid crystalline behaviour by the formation of binary mixtures of the carbazole derivatives with TNF, which has been shown[16] to induce liquid crystalline behaviour in other disc-shaped materials which alone do not display

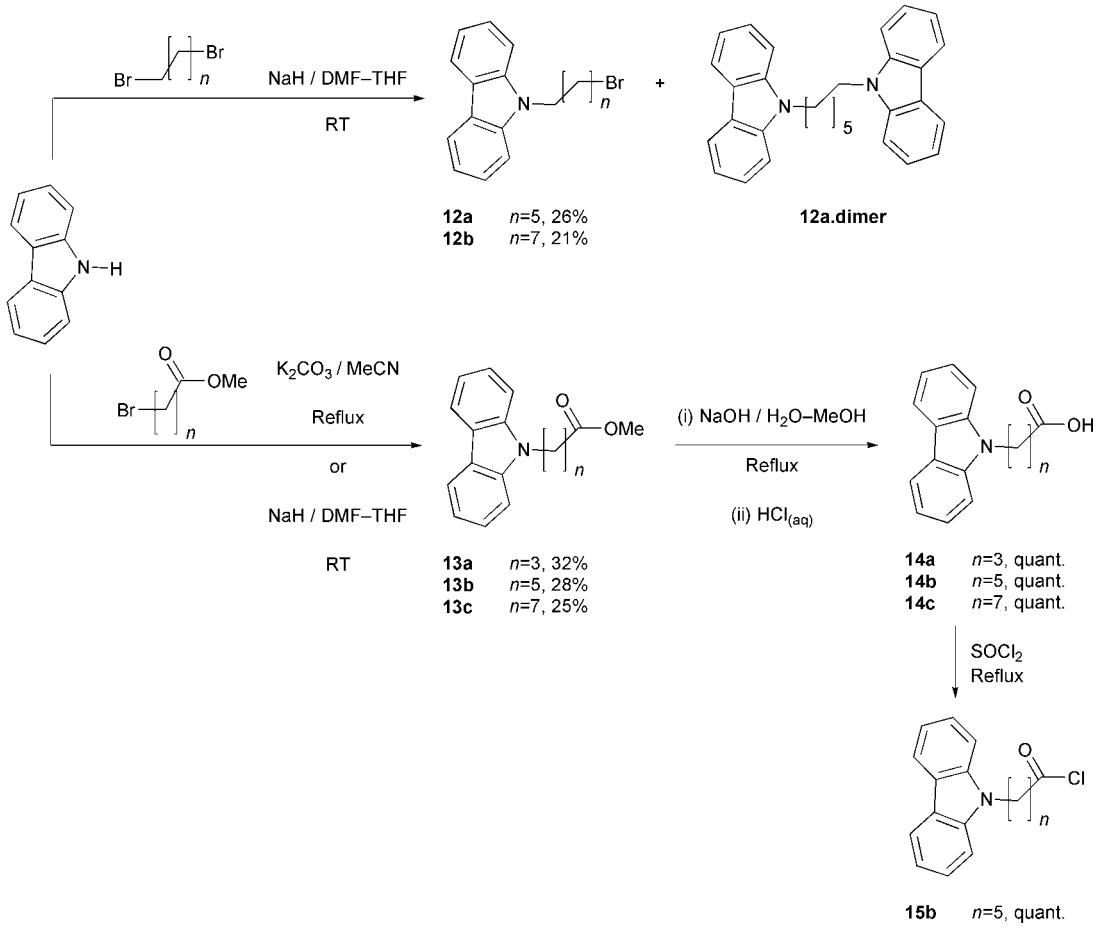

Scheme 2 Synthetic routes to the carbazole derivatives **12a–b**, **14a–c** and **15b** used in the coupling with **7–11**.

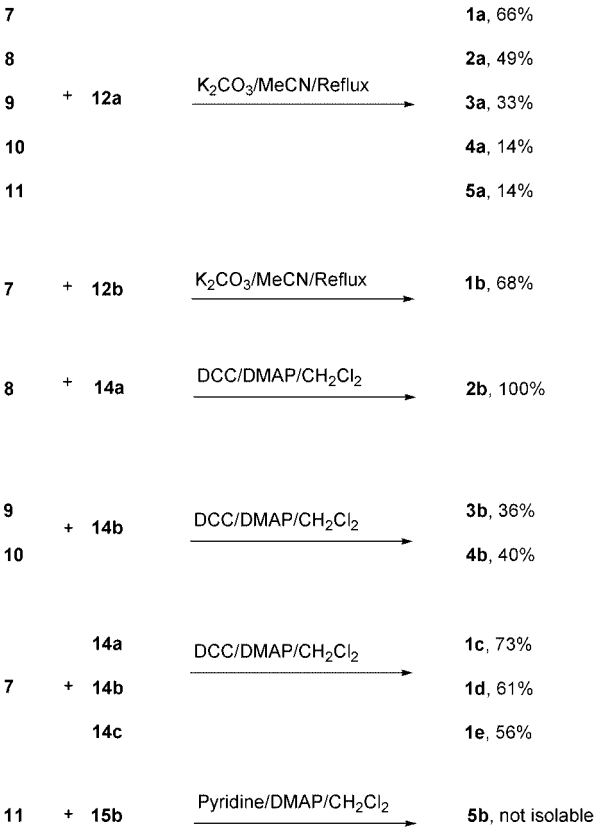

Scheme 3 Synthetic routes to target carbazole derivatives **1–5**.

mesophases. Initial screening was performed by variable temperature optical polarised microscopy by contact preparation of the carbazole materials with TNF. This revealed that for the monocarbazole derivatives **1a–d**, a mesophase could be induced at the boundary between the molten materials (Fig. 2 illustrates the OPM picture for **1c**–TNF contact preparation). Induction of mesophases could also be achieved for the bis-carbazole derivatives **2a** and **2b**. However, none of the higher substituted derivatives (**3–5**) displayed a mesophase with TNF by contact preparation.

A quantitative investigation of the mesophase behaviour of **1a–e**, **2a** and **2b** as function of the mol% of TNF in the binary mixtures is tabulated in Tables 1 and 2, whilst Fig. 3 graphically illustrates these data for compounds **1a–e**. Fig. 4 illustrates the mesophase textures of **1a** with various doping concentrations of TNF. All of the mesophase textures were indicative of a Col_h ordering, displaying droplets with linear defects as well as homeotropic star-shaped domains with hexagonal symmetry domains which developed into a mosaic texture upon cooling from the isotropic melt.[21] The Col_h structure was confirmed by X-ray diffraction experiments (see later). The doped samples were prepared from a solution of the colourless carbazole derivative[16] with the appropriate equivalent of the pale yellow solutions of TNF followed by concentration *in vacuo* to leave dark brown residues which were further rigorously dried on a vacuum line. Upon heating, these samples passed directly from the solid state into the isotropic liquid state. However, upon cooling they passed from the isotropic liquid state to a birefrigent liquid state whose textures were indicative of hexagonal columnar mesophases. These phase changes were confirmed by X-ray crystallography. All of the mesophases persisted down to room temperature, and the mesophases even survived storage in the fridge for two hours without crystallisation. Mixtures containing more than

Table 1 Phase behaviour of binary mixtures of the carbazole derivatives **1a–e** and TNF as a function of temperature as determined by optical polarising microscopy and X-ray analysis

	Phase behaviour				
TNF/mol%	**1a**	**1b**	**1c**	**1d**	**1e**
0.0	K 106 °C I	K 72 °C I	K 77 °C I	K 99 °C I	K 78 °C I
2.3	K 81 °C I	K 73 °C I	K 79 °C I	K 62 °C I	K 95 °C I
4.9	K 74 °C I	K 80 °C I	I 110 °C[a] Col_h	I 77 °C[a] Col_h	K 98 °C I
9.5	K 80 °C I	K 71 °C I	I 142 °C Col_h	I 96 °C Col_h	K 70 °C I
16.6	I 82 °C Col_h	I 66 °C Col_h	—	—	—
23.1	I 130 °C Col_h	I 99 °C Col_h	I 185 °C Col_h	I 150 °C Col_h	I 90 °C Col_h
32.9	I 144 °C Col_h	I 113 °C Col_h	I 190 °C Col_h	I 153 °C Col_h	I 116 °C Col_h
41.1	I 150 °C Col_h	I 114 °C Col_h	I 189 °C Col_h	I 152 °C Col_h	I 115 °C Col_h
50.0	I 139 °C Col_h	I 96 °C Col_h	I 179 °C Col_h	I 111 °C Col_h	I 70 °C Col_h
66.8	K 147 °C I	K 145 °C I	K 70 °C I	K 107 °C I	K 99 °C I

[a]The mesophase texture was not very well-defined at this mol% of TNF.

Table 2 Phase behaviour of the carbazole derivatives **2–5** as a function of temperature and doping 1 : 1 with TNF as determined by optical polarising microscopy

	Phase behaviour							
TNF/ mol%	**2a**	**2b**	**3a**	**3b**	**4a**	**4b**	**5a**	**5b**
0	K 114 °C I	K 147 °C I	K 132 °C I	K 106 °C I	K 122 °C I	K 104 °C I	K 89 °C I	K 290 °C (dec)
50	I 90 °C Col_h	I 112 °C Col_h	No mesophase[a]	No mesophase[a]	No mesophase[a]	No mesophase[a]	No mesophase[a]	No mesophase[a]

[a]As determined by contact preparation.

50 mol% TNF are thermodynamically unstable due to phase separation by crystallization of TNF.

Detailed analysis of Tables 1 and 2 and Fig. 3 reveals that: (a) for both the ether linked samples **1a** and **1b** and the ester linked samples **1c–e**, an increase in the length of the spacer between the triphenylene moiety and the carbazole unit reduces the isotropization temperature (Fig. 3a); (b) the replacement of the methylene unit for the carbonyl unit when comparing **1a** with **1d** (C_6 chains), and **1b** with **1e** (C_8 chains): (i) has little effect of the isotropization temperatures in the range between 23.1 to 41.1 mol% of TNF (the largest difference is 20 °C for 23.1 mol% doping when comparing **1a** and **1d**, and all other differences in the range are 10 °C or less) (Fig. 3b), (ii) increases the doping concentration over which the mesophases are observed when comparing **1b** and **1e**, but decreases when comparing **1a** and **1d** (Fig. 3b), and (iii) results in a reversal in the clearing temperature sequence for the highest TNF doping concentration (50 mol %) at which the mesophases were observed such that **1a** and **1b** have the higher clearing temperature (Fig. 3b) relative to **1d** and **1e**, respectively; (c) the highest clearing temperature is observed in every case in the region of 30–40 mol% TNF, which is suggestive of a "2 : 1 complex" in which each π-electron deficient TNF molecule is sandwiched between two π-electron rich triphenylene–carbazole moieties.

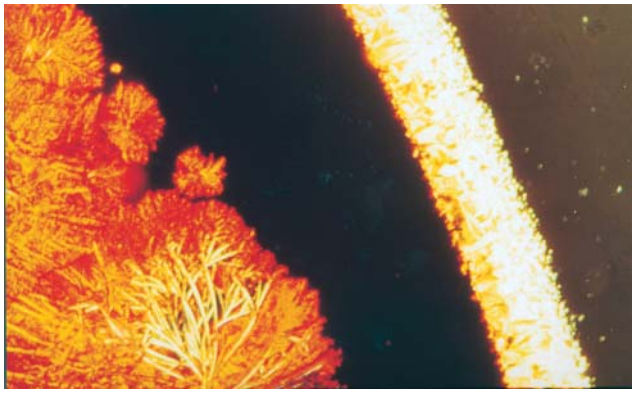

Fig. 2 Optical polarising micrograph of contact preparation experiment of **1c** and TNF.

Thus, it can be summarised that chain length governs isotropization of the mesophases, whilst the nature of the linking group (ether, -OCH_2-, or ester, -OC(O)-) governs the range of concentrations with which TNF can induce the mesophases, with a maximum stabilisation indicative of a 2 : 1 complex structure. We speculate here that the more polar ester functionality in **1c** and **1d** interacts with the polar TNF moiety in such a way that at lower concentrations of TNF doping, the TNF is intercalated more easily between the electron rich π-units of the triphenylene moieties and/or the carbazole units and in turn induces the mesophase at lower concentrations, relative to the less polar ether linked derivatives **1a** and **1b**.

2.4 UV Analysis

In order to ascertain with which π-donor unit (carbazole or triphenylene) the TNF forms the charge-transfer complex, solution state UV/Vis experiments were carried out with **1a**, the carbazole derivative **12a**, hexakis(pentyloxy)triphenylene derivative **6a** and TNF. The UV/Vis spectra of the 1 : 1 mixtures (10^{-2} M) of **1a**, **12a**, and **6a** with TNF revealed that there was only a small CT band associated with the carbazole **12a**–TNF interaction, with a λ_{max} at 450 nm ($\varepsilon = 75\ M^{-1}\ cm^{-1}$), whereas with **6a**–TNF there was a much stronger band at a λ_{max} onset at 620 nm ($\varepsilon = 300\ M^{-1}\ cm^{-1}$). Thus, it was not unexpected that the CT band of **1a** with TNF resembled that of **6a**–TNF with the λ_{max} onset at 570 nm ($\varepsilon = 250\ M^{-1}\ cm^{-1}$). Thus, it was concluded that in solution the CT complex between **1a** and TNF results primarily from the triphenylene moiety–TNF interaction. This conclusion was extrapolated to the condensed phase by the visual appearance of the binary materials, which resembled the colours of the solutions.

2.5 X-Ray diffraction

X-Ray diffraction experiments have been carried out on two compounds (**1b** and **1c**) as complex mixtures with 32.9 mol% and 50 mol% TNF) at 30 °C and 100 °C in their mesophase

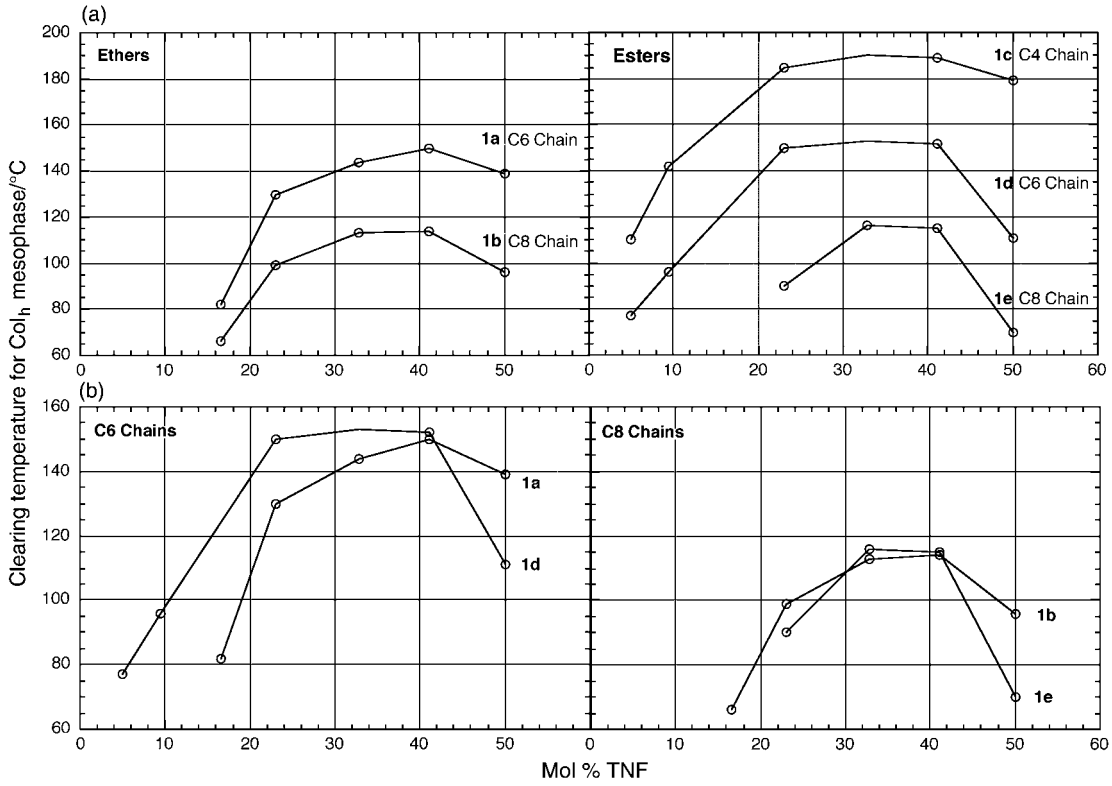

Fig. 3 (a) Graphical representation of the monotropic behaviour of the ether linked carbazole derivatives **1a** and **1b** as binary mixtures with varying concentrations of TNF, and the ester linked carbazole derivatives **1c**–**e** as binary mixtures with varying concentrations of TNF as they enter the hexagonal columnar mesophase from the isotropic liquid. (b) Graphical representation to compare and contrast the thermal behaviour of the Col$_h$ mesophases as a function of the ether linkage and the ester linkage for the carbazole units separated by C_6 (**1a** and **1d**) chains and C_8 (**1b** and **1e**) chains from the triphenylene moieties.

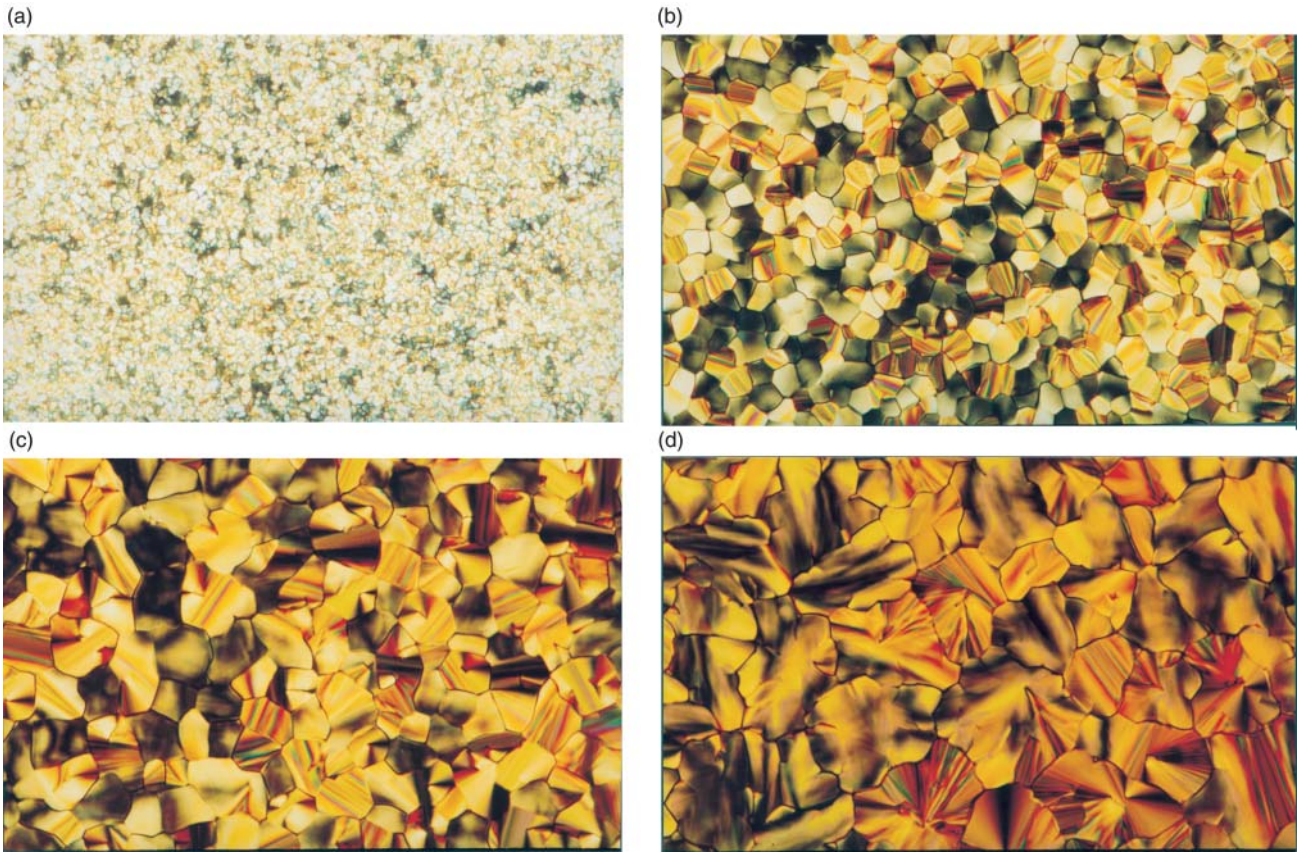

Fig. 4 Optical polarising micrographs of **1a** with TNF in the Col$_h$ mesophase (a) 2.3 mol%, (b) 9.5 mol%, (c) 32.9 mol%, and (d) 41.1 mol% of TNF.

Table 3 X-Ray diffraction data for compounds **1b** and **1c** with 32.9 mol% and 50 mol% TNF in the Col_h mesophase at 30 °C and 50 °C, and 30 °C and 100 °C, respectively

Compound	TNF/mol%	Temp./°C	*d*-Spacings/nm			Columnar spacing/nm	Correlation length/nm
			d_{100}	$d_{core-core}$	d_{alkyl}		
1b	32.9	30	1.86	0.339	0.434	2.14	13.39
1b	50.0	30	1.74	0.336	0.430	2.01	13.10
1b	32.9	50	1.86	0.340	0.438	2.14	11.80
1b	50.0	50	1.75	0.336	0.434	2.02	10.68
1c	32.9	30	1.79	0.339	0.432	2.07	12.09
1c	50.0	30	1.71	0.337	0.429	1.97	14.26
1c	32.9	100	1.81	0.343	0.444	2.09	10.47
1c	50.0	100	1.74	0.340	0.438	2.01	11.47

ranges, the results of which are shown in Table 3. The features of the diffractograms for all combinations of molar ratio and temperature were similar. As a representative example, we describe in detail the case for **1c** at 100 °C in a 1 : 1 ratio with TNF. The diffraction pattern (Fig. 5a) and the derived one-dimensional intensity *versus* 2θ profile (Fig. 5b) obtained by integrating over the entire χ (0–360°) range at 100 °C, are consistent with the structure of a Col_h mesophase. In the low angle region, four sharp peaks (one strong and three weak reflections) are observed whose *d*-spacings are in the ratio $1:1\sqrt{3}, 1:1\sqrt{4}$, and $1:1\sqrt{7}$. Indentifying the first peak with the Miller index (100), the ratios conform to the expected values from a two-dimensional hexagonal lattice. In the wide angle region, two diffuse reflections are observed. The broad one corresponds to the liquid-like ordering of the aliphatic chains, whilst the relatively sharper one, observed at higher 2θ values and well separated from the broad one, is due to the stacking of the triphenylene cores in a columnar fashion. Similar features were observed for the scans taken at 30 °C.

For all substances studied, the core–core separation at 30 °C was in the range 0.336–0.340 nm. These values are about 0.02 nm shorter than those observed in undoped triphenylene mesophases, but are comparable to the values for TNF doped triphenylene mesophases. Thus, the core–core separation for **1b** decreases from 0.339 nm (33 mol% TNF) to 0.336 nm (50 mol% TNF) at 30 °C and from 0.340 nm to 0.336 nm at 100 °C. These results are indicative of increased core–core interactions in the columns as the mole ratio of TNF is increased in the binary mixtures. Additionally, the core–core separation was found to be weakly temperature dependent, such that at higher temperatures, the separation increased as would be expected.

However, an unusual result from the X-ray analysis is depicted in Fig. 6. The results for the ester **1c** are as expected, *i.e.* as the mol% of TNF increases, the correlation length increases at both 30 °C and 100 °C, suggesting closely packed columnar structure. However, although the core–core separation decreases with increasing mol% of TNF for the ether **1b**, the correlation length decreases at both temperatures. Thus, the polar C=O bond in the ester derivative must also be playing an important role in the stabilisation of the mesophase. This conclusion fits with a recent study of mixed ether–ester triphenylene derivatives which have shown higher correlation length compared to pure triphenylene ethers.[22]

3 Concluding remarks

The synthesis of several mesogenic carbazole derivatives has been described. The pure compounds were found not to be liquid crystalline in nature. However, by doping with TNF, mesophases were induced with optical textures associated with columnar ordering. These were subsequently confirmed by X-ray diffraction as being Col_h. The highest clearing points as a function of TNF doping suggest that a 2 : 1 complex structure is formed between the triphenylene–carbazole materials (**1a**–**1e**) and the TNF, respectively. Liquid crystalline carbazole derivatives are proposed as superior photorefractive materials to the amorphous polymeric carbazole materials, as a consequence of their inherent anisotropic ordering. Additionally, the doping of the materials described here with TNF, is advantageous and fortuitous, as it is reported[11] that TNF enhances the photorefractive properties of the polymeric materials studied to date.[11]

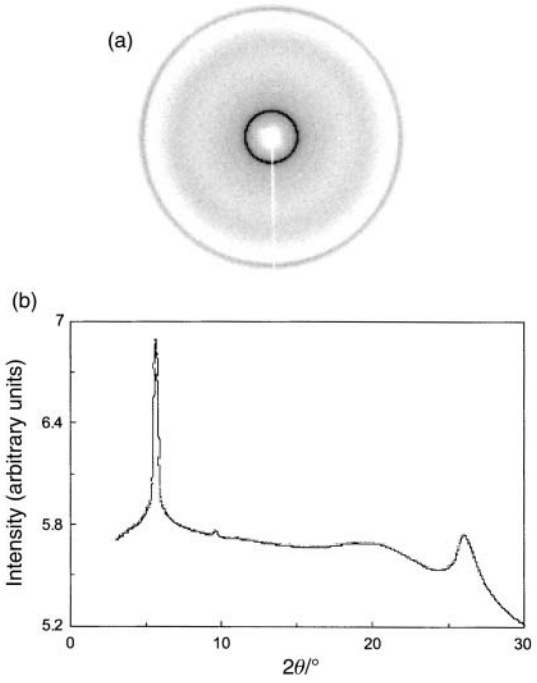

Fig. 5 X-Ray diffraction data for **1c** with 50 mol% of TNF at 100 °C; (a) diffraction pattern, and (b) one dimensional intensity profile *versus* 2θ.

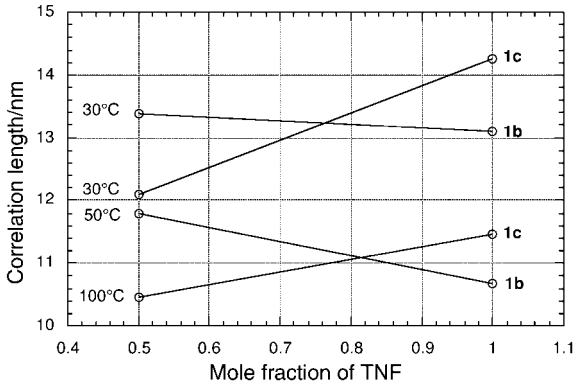

Fig. 6 Plots of correlation lengths (from X-ray diffraction data) *versus* mol ratio TNF for **1b** and **1c** at 30 °C and 100 °C.

Currently, we are also synthesising and characterising various series of mono-, tris-, and hexakis-functionalised carbazole triphenylene derivatives and investigating their thermal behaviour also as CT complexes with TNF, as well as the introduction of the carbazole moiety into banana-shaped molecular structures.[23] These next generation materials are functionalised to induce push–pull electronic systems for NLO behaviour, photorefractive properties and ferroelectric switching.

4 Experimental

General methods

Most of the reactions were carried out under a nitrogen atmosphere. Chemicals were purchased from Aldrich and used as received. Yields refer to chromatographically pure products. Thin-layer Chromatography (TLC) was carried out on aluminium sheets coated with silica gel 60 (Merck 5554 mesh). Column chromatography was performed on silica gel 60 (Merck 230-400). Microanalyses were performed by the University of London microanalytical laboratories or by the University of Birmingham microanalytical services. Electron impact (EI) mass spectra were recorded at 70eV on a VG ProSpec mass spectrometer. Liquid secondary ion mass spectra (LSIMS) were recorded on a VG ZabSpec mass spectrometer equipped with a caesium ion source utilising *m*-nitrobenzyl alcohol containing a trace of sodium acetate as the matrix.^{1}H NMR spectra were recorded on a Bruker AC 300 (300 MHz) or a Bruker AMX400 (400 MHz) or a Bruker DRX500 (500 MHz) spectrometer.^{13}C NMR spectra were recorded on a Bruker AC300 (75.5 MHz) or a Bruker DRX500 (125.8 MHz) spectrometer. The chemical shift values are expressed as δ values and the coupling constant values (J) are in hertz. The following abbreviations are used for the signal multiplicities or characteristics: s, singlet; d, doublet; dd, double doublet; t, triplet; m, multiplet; q, quartet; quint; quintet; br, broad. Transition temperatures were measured using a Mettler FP82 HT hot stage and central processor in conjunction with Leitz DMFRT polarizing mircroscope as well as differential scanning calorimetry (DSC7 Perkin-Elmer).

X-Ray studies were performed using an image plate detector (MAC Science DIP 1030). Unoriented samples contained in sealed Lindemann glass capillaries were irradiated with CuKα rays obtained from a sealed-tube generator (Enraf-Nonius FR590) in conjunction with double mirror focusing optics. 2,3,6,7,10,11-Hexakis(pentyloxy)triphenylene (**6a**),[19] 2-hydroxy-3,6,7,10-pentakis(pentyloxy)triphenylene (**7**),[17] hexamethoxytriphenylene (**6b**),[18] 2,7-dihydroxy-3,6,10,11-tetrakis(pentyloxy)triphenylene (**8**),[17] symmetrical 2,6,10-trihydroxy-3,7,11-tris(pentyloxy)triphenylene (**9**)[17] asymmetrical 2,7,10-trihydroxytris(pentyloxy)triphenylene (**10**),[17] and hexahydroxytriphenylene (**11**)[18] were synthesized according to literature procedures. The charge transfer complexes of the carbazole triphenylene derivatives (**1a**–**2b**), with TNF were prepared by dissolving the appropriate amount of both compounds separately in CH_2Cl_2, mixing the solutions and evaporating the solvent.[24] X-Ray studies were performed using an image plate detector (MAC Science DIP 1030) as described previously.[25]

Compound 1a

A solution of 2-hydroxy-3,6,7,10-pentakis(pentyloxy)triphenylene **7** (0.50 g, 0.74 mmol) in DMSO (25 mL) was added to K_2CO_3 (0.20 g, 1.48 mmol). The resultant slurry was stirred and heated under reflux. A solution of bromocarbazole **12a** (0.29 g, 0.8 mmol) in DMSO (5 mL) was added dropwise over a few minutes to the slurry, maintaining heating under reflux. Heating was continued overnight. The reaction mixture was cooled, H_2O (20 mL) was added, and the reaction mixture was extracted with Et_2O (2 × 25 mL). The combined organic extracts were dried ($MgSO_4$), filtered, and the filtrate evaporated to dryness under reduced pressure. The residue was purified by silica gel column chromatograpy (eluent: hexane–CH_2Cl_2, 1 : 3) to afford **1a** (0.450 g, 66%) as a white solid: ^{1}H NMR (300 MHz, $CDCl_3$, 21 °C): δ = 0.95 (m, 15 H), 1.48 (m, 2 H), 1.92 (m, 14 H), 4.20 (m, 12 H), 4.35 (t, J = 7.0 Hz, 2 H), 7.21 (m, 2 H), 7.44 (m, 4 H), 7.82 (m, 6 H), 8.09 (d, J = 7.7 Hz, 2 H); ^{13}C NMR (75 MHz, $CDCl_3$, 21 °C): δ = 14.0, 22.5, 26.0, 27.1, 28.8, 29.0, 29.1, 29.3, 43.0, 69.4, 69.6, 69.7, 69.8, 107.3, 107.4, 107.5, 107.6, 108.6, 118.9, 120.3, 122.8, 123.6, 123.7, 125.6, 140.4, 148.9, 149.0; MS (LSIMS): *m*/*z* 924 $[M + H]^+$; elemental analysis calcd (%) for $C_{61}H_{81}O_6N$: C 79.30, H 8.77, N 1.51; found C 79.30, H 8.58, N 1.46.

The same procedure for **1a** was followed for the synthesis of **1b**, **2a**, **3a**, **4a** and **5a**. (Quantities used for this set of reactions are displayed in Table 1 of the supplementary material.‡)

Compound 1b. ^{1}H NMR (500 MHz, $CDCl_3$, 31 °C): δ = 1.05–1.00 (m, 15 H), 1.55–1.47 (m, 14 H), 1.65–1.57 (m, 14 H), 2.03–1.88 (m, 14 H), 4.29–4.23 (m, 14 H), 7.24 (br t, J = 7.3 Hz, 2 H), 7.48 (br d, J = 7.2 Hz, 2 H), 7.47 (br t, J = 7.7 Hz, 2 H), 7.89 (br s, 6 H), 8.12 (d, J = 7.7 Hz, 2 H); ^{13}C NMR (125 MHz, $CDCl_3$, 31 °C): δ = 14.0, 22.5, 26.0, 27.2, 28.3, 28.9, 29.1, 29.3, 29.3, 29.4, 42.9, 69.7, 107.4, 108.5, 118.6, 120.2, 122.8, 123.6, 125.5, 140.3, 149.0; MS (LSIMS): *m*/*z* 952 $[M + H]^+$; elemental analysis calcd (%) for $C_{63}H_{85}NO_6$: C 79.49, H 8.93, N 1.47; found C 79.46, H 8.80, N 1.52.

Compound 2a. ^{1}H NMR (500 MHz, $CDCl_3$, 31 °C): δ = 1.01–0.96 (q, J = 14.2, 7.2 Hz, 12 H), 1.56–1.43 (m, 6 H), 1.62–1.54 (m, 14 H), 1.69–1.63 (m, 4 H), 1.99–1.94 (m, 16 H), 4.26–4.21 (m, 12 H), 4.34 (t, J = 7.1 Hz, 4 H), 7.25–7.22 (m, 4 H), 7.48–7.42 (m, 8 H), 7.86 (br s, 6 H), 8.11 (d, J = 7.6 Hz, 4 H); ^{13}C NMR (125 MHz, $CDCl_3$, 31 °C): δ = 14.0, 22.4, 22.5, 25.9, 27.0, 28.3, 28.9, 29.0, 29.1, 29.3, 42.8, 69.4, 69.6, 69.7, 107.3, 107.4, 107.5, 108.5, 118.7, 120.2, 122.8, 123.6, 125.5, 140.3, 148.9, 148.9, 149.0; MS (LSIMS): *m*/*z* 1103 $[M + H]^+$; elemental analysis calcd (%) for $C_{74}H_{90}N_2O_6$: C 80.58, H 8.16, N 2.54; found C 79.86, H 8.11, N 2.65.

Compound 3a. ^{1}H NMR (300 MHz, $CDCl_3$, 21 °C): δ = 0.9 (t, J = 7.3 Hz, 9 H), 1.53 (m, 24 H), 1.92 (m, 18 H), 4.15 (m, 12 H), 4.33 (t, J = 6.9 Hz, 6 H), 7.20 (m, 6 H), 7.42 (br s, 6 H), 7.43 (m, 6 H), 7.80 (br s, 6 H), 8.08 (d, J = 7.7 Hz, 6 H); ^{13}C NMR (75 MHz, $CDCl_3$, 21 °C): δ = 14.0, 22.4, 25.9, 27.1, 28.3, 28.9, 29.0, 29.3, 42.9, 69.4, 69.7, 107.4, 107.5, 108.5, 118.7, 120.3, 122.8, 123.6, 123.7, 125.5, 140.4, 148.9, 149.0; MS (LSIMS): *m*/*z* 1283 $[M + H]^+$; elemental analysis calcd (%) for $C_{87}H_{99}N_3O_6$: C 81.42, H 7.72, N 3.26; found C 81.49, H 7.92, N 3.28.

Compound 4a. ^{1}H NMR (500 MHz, $CDCl_3$, 21 °C): δ = 0.94–0.89 (m, 9 H), 1.45–1.37 (m, 6 H), 1.55–1.47 (m, 12 H), 1.66–1.58 (m, 6 H), 1.97–1.84 (m, 18 H), 4.21–4.15 (m, 12 H), 4.33–4.28 (m, 6 H), 7.21–7.17 (m, 6 H), 7.44–7.37 (m, 12 H), 7.79 (br s, 2 H), 7.80 (br s, 2 H), 7.82 (br s, 2 H), 8.08–8.06 (m, 6 H); ^{13}C NMR (125 MHz, $CDCl_3$, 31 °C): δ = 14.1, 22.5, 25.9, 27.1, 28.3, 28.9, 29.1, 29.3, 42.9, 69.4, 69.5, 69.6, 107.3, 107.4, 107.5, 107.6, 108.6, 118.7, 120.3, 122.8, 123.6, 123.7, 125.5, 140.4, 148.9, 149.0; MS (LSIMS); *m*/*z* 1283 $[M + H]^+$; elemental analysis calcd (%) for $C_{87}H_{99}N_3O_6$: C 81.42, H 7.72, N 3.26; found C 81.42, H 7.83, N 3.26.

Compound 5a. ^{1}H NMR (500 MHz, $CDCl_3$, 31 °C): δ = 1.43–1.37 (m, 12 H), 1.57–1.51 (m, 12 H), 1.86–1.78 (m, 24 H), 4.11 (t, J = 12.6 Hz, 12 H), 4.2 (t, J = 14.3 Hz, 12 H), 7.16 (ddd, J = 7.83, 0.8, 1.0 Hz, 12 H), 7.03 (d, J = 8.1 Hz, 12 H), 7.39 (ddd, J = 8.1, 1.1, 1.1 Hz, 12 H), 7.76 (br s, 6 H), 8.04

(d, J = 7.7 Hz, 12 H); ^{13}C NMR (125 MHz, $CDCl_3$, 31 °C): δ = 25.9, 27.0, 28.9, 29.3, 42.8, 69.4, 107.5, 108.6, 118.7, 120.3, 122.8, 123.7, 125.6, 140.4, 148.9; MS (LSIMS): m/z 1820 $[M + H]^+$; elemental analysis calcd (%) for $C_{126}H_{126}N_6O_6$: C 83.16, H 6.93, N 4.62; found C 83.21, H 6.90, N 5.01.

Compound 1c

To a solution of the carbazole derivative **14a** (0.22 g, 0.89 mmol) in dry CH_2Cl_2 (10 mL), cooled to 0 °C under a N_2 atmosphere, was added 1,3-dicyclohexylcarbodiimide (0.18 g, 0.89 mmol) and a catalytic amount of 4-dimethylaminopyridine. The mixture was stirred for 30 minutes and 2-hydroxy-3,6,7,10-pentakis(pentyloxy)triphenylene **7** (0.50 g, 0.74 mmol) was added over 10 minutes, followed by further stirring for 24 hours under a N_2 atmosphere at room temperature. The white precipitate was filtered and the filtrate was diluted with CH_2Cl_2 (30 mL) and washed with H_2O (3 × 30 mL), followed by 10% $NaHCO_3$ (10 mL) and brine (5 mL). The organic phase was dried over ($MgSO_4$), filtered, and the filtrate evaporated to dryness under reduced pressure. The residue was purified by silica gel column chromatography (eluent: hexane–CH_2Cl_2, 1 : 3) to yield **1c** (0.49 g, 73%) as a white solid: ^{1}H NMR (500 MHz, $CDCl_3$, 31 °C): δ = 0.91 (t, J = 7.2 Hz, 6 H), 1.02–0.98 (m, 9 H), 1.41–1.34 (m, 2 H), 1.50–1.45 (m, 10 H), 1.60–1.55 (m, 8 H), 1.88–1.82 (m, 6 H), 2.00–1.95 (m, 4 H), 2.44–2.30 (m, 2 H), 2.76 (t, J = 7.0 Hz, 2 H), 4.25–4.21 (m, 10 H), 4.54 (t, J = 7.0 Hz, 2 H), 7.28–7.25 (m, 2 H), 7.53–7.48 (m, 4 H), 7.78 (br s, 1 H), 7.83 (br s, 2 H), 7.87 (br s, 2 H), 8.06 (br s, 1 H), 8.14 (d, J = 7.7 Hz, 2 H); ^{13}C NMR (125 MHz, $CDCl_3$, 31 °C): δ = 3.9, 14.0, 22.3, 22.5, 24.1, 28.1, 28.3, 28.9, 29.0, 29.1, 31.0, 41.8, 68.7, 69.2, 69.4, 69.7, 69.8, 106.0, 106.6, 106.9, 107.3, 108.0, 108.6, 116.5, 118.9, 120.3, 122.9, 123.1, 123.2, 123.4, 124.6, 125.7, 128.0, 139.5, 140.3, 148.8, 149.0, 149.2, 149.7, 171.1; IR (Nujol): ν = 1617 cm^{-1} (C=O); MS (LSIMS): m/z 910 $[M + H]^+$; elemental analysis calcd (%) for $C_{59}H_{75}NO_7$: C 77.88, H 8.25, N 1.54; found C 77.72, H 8.33, N 1.51.

The same procedure for **1c** was followed for the synthesis of **1d**, **1e**, **2b**, **3b** and **4b**. (Quantities used for these esterification reactions are shown in Table 2 of the supplementary material.‡)

Compound 1d. ^{1}H NMR (500 MHz, $CDCl_3$, 31 °C): δ = 1.50–1.40 (m, 15 H), 1.53–1.40 (m, 12 H), 1.63–1.55 (m, 12 H), 2.02–1.85 (m, 14 H), 2.66 (t, J = 7.4 Hz, 2 H), 4.22–4.17 (m, 10 H), 4.32 (t, J = 7.1 Hz, 1 H), 7.25 (ddd, J = 7.8, 0.8, 0.9 Hz, 2 H), 7.42 (d, J = 8.1 Hz, 2 H), 7.49 (ddd, J = 7.8, 0.8, 0.9 Hz, 2 H), 7.76 (br s, 1 H), 7.80 (br s, 2 H), 7.82 (br s, 1 H), 7.83 (br s, 1 H), 8.04 (br s, 1 H), 8.11 (d, J = 7.7 Hz, 2 H); ^{13}C NMR (125 MHz, $CDCl_3$, 31 °C): δ = 14.0, 22.4, 22.5, 24.7, 26.7, 28.1, 28.3, 28.6, 28.9, 29.0, 29.1, 33.8, 42.6, 68.6, 69.1, 69.3, 69.6, 69.7, 105.9, 106.5, 106.8, 107.2, 107.9, 108.4, 116.5, 118.7, 120.2, 122.8, 122.9, 123.0, 123.1, 123.3, 124.5, 125.5, 127.8, 139.6, 140.3, 148.1, 148.8, 149.1, 149.2, 149.6, 171.5; IR (Nujol): ν = 1613 cm^{-1} (C=O); MS (LSIMS): m/z 938 $[M + H]^+$; elemental analysis calcd (%) for $C_{61}H_{79}NO_7$: C 78.12, H 8.43, N 1.49; found C 78.31, H 8.54, N 1.36.

Compound 1e. ^{1}H NMR (500 MHz, $CDCl_3$, 31 °C): δ = 1.05–0.98 (m, 15 H), 1.53–1.44 (m, 14 H), 1.65–1.58 (m, 12 H), 2.01–1.83 (m, 14 H), 2.68 (t, J = 7.5 Hz, 2 H), 4.32–4.19 (m, 12 H), 7.25 (br t, J = 7.4 Hz, 2 H), 7.42 (br d, J = 8.1 Hz, 2 H), 7.48 (br t, J = 7.5 Hz, 2 H), 7.77 (br s, 1 H), 7.81 (br s, 2 H), 7.84 (br d, J = 7.0 Hz, 2 H), 8.06 (s, 1 H), 8.12 (d, J = 7.7 Hz, 2 H); ^{13}C NMR (125 MHz, $CDCl_3$, 31 °C): δ = 14.0, 22.5, 24.9, 27.1, 28.1, 28.3, 28.9, 28.9, 29.1, 29.1, 34.0, 42.9, 68.6, 69.2, 69.4, 69.7, 69.8, 105.9, 106.6, 106.8, 107.2, 107.9, 108.5, 116.5, 118.6, 120.2, 122.7, 122.9, 123.0, 123.1, 123.4, 124.5, 125.5, 127.8, 139.7, 140.3, 148.7, 148.9, 149.1, 149.3, 149.6, 171.7; IR (Nujol): ν = 1614, 1745 cm^{-1} (C=O); MS (LSIMS): m/z 966 $[M + H]^+$; elemental analysis calcd (%) for $C_{63}H_{83}NO_7$: C 78.34, H 8.60, N 1.45; found C 78.43, H 8.59, N 1.65.

Compound 2b. ^{1}H NMR (500 MHz, $CDCl_3$, 31 °C): δ = 0.99 (t, J = 7.2 Hz, 6 H), 1.0–1.2 (m, 6 H), 1.39–1.32 (m, 4 H), 1.50–1.52 (m, 8 H), 1.58–1.53 (m, 4 H), 1.87–1.81 (m, 4 H), 1.97–1.91 (m, 4 H), 2.44–2.38 (m, 4 H), 2.75 (t, J = 7.0 Hz, 4 H), 4.23–4.19 (m, 8 H), 4.54 (t, J = 7.0 Hz, 4 H), 7.28–7.25 (m, 4 H), 7.53–7.47 (m, 8 H), 7.70 (br s, 2 H), 7.86 (br s, 2 H), 8.04 (br s, 2 H), 8.14 (d, J = 7.7 Hz, 4 H); ^{13}C NMR (125 MHz, $CDCl_3$, 31 °C): δ = 13.9, 14.0, 22.3, 22.5, 24.1, 28.1, 28.3, 28.9, 29.0, 31.0, 41.9, 68.8, 69.1, 69.3, 69.4, 106.4, 106.6, 108.6, 116.7, 119.0, 120.4, 122.9, 124.1, 125.7, 127.4, 140.3, 149.2, 149.2, 171.1; IR (Nujol): ν = 1620, 1752 cm^{-1} (C=O); MS (LSIMS): m/z 1075 $[M + H]^+$; elemental analysis calcd (%) for $C_{70}H_{78}N_2O_8$: C 78.21, H 7.26, N 2.60; found C 78.37, H 7.37, N 2.80.

Compound 3b. ^{1}H NMR (500 MHz, $CDCl_3$, 31 °C): δ = 0.94 (t, J = 7.2 Hz, 9 H), 1.43–1.78 (m, 6 H), 1.50–1.45 (m, 6 H), 1.64–1.58 (m, 6 H), 1.85–1.79 (m, 6 H), 1.95–1.88 (m, 6 H), 2.03–1.97 (m, 6 H), 2.63 (t, J = 8.0 Hz, 6 H), 4.08 (t, J = 6.8 Hz, 6 H), 4.34 (t, J = 7.1 Hz, 6 H), 7.28–7.23 (ddd, J = 7.8 , 1.0, 0.9 Hz, 6 H), 7.51–7.48 (ddd, J = 7.0, 1.1, 1.0 Hz, 9 H), 7.44 (d, J = 8.1 Hz, 6 H), 7.86 (br s, 3 H), 8.13 (d, J = 7.7 Hz, 6 H); ^{13}C NMR (125 MHz, $CDCl_3$, 31 °C): δ = 14.0, 22.5, 25.0, 26.8, 28.1, 28.7, 29.1, 34.0, 42.7, 68.1, 105.8, 108.5, 117.5, 118.8, 120.3, 122.0, 122.9, 125.6, 128.2, 139.1, 140.3, 149.3, 171.6; IR (Nujol): ν = 1595, 1622, 1748 cm^{-1} (C=O); MS (LSIMS): m/z 1324 $[M + H]^+$; elemental analysis calcd (%) for $C_{87}H_{93}N_3O_9$: C 78.91, H 7.02, N 3.17; found C 78.82, H 7.08, N 3.32.

Compound 4b. ^{1}H NMR (500 MHz, $CDCl_3$, 31 °C): δ = 1.03–0.98 (m, 9 H), 1.49–1.43 (m, 6 H), 1.59–1.52 (m, 6 H), 1.66–1.59 (m, 6 H), 1.97–1.84 (m, 10 H), 2.05–1.99 (m, 8 H), 2.71–2.64 (m, 6 H), 4.22–4.13 (m, 6 H), 4.35 (ABq, J = 12.6, 6.9 Hz, 6 Hz), 7.32–7.29 (m, 6 H), 7.46 (br d, J = 8.1 Hz, 6 H), 7.53 (ddd, J = 8.1, 1.0, 1.0 Hz, 6 H), 7.61 (s, 1 H), 7.71 (s, 1 H), 7.73 (s, 1 H), 7.76 (s, 1 H), 7.79 (s, 1 H), 7.99 (s, 1 H), 8.16 (br d, J = 0.7 Hz, 3 H), 8.18 (br d, J = 0.8 Hz, 3 H); ^{13}C NMR (125 MHz, $CDCl_3$, 31 °C): δ = 14.0, 22.4, 24.7, 26.7, 28.1, 28.2, 28.6, 28.9, 33.8, 42.6, 68.4, 68.5, 68.6, 105.7, 106.2, 106.3, 108.4, 116.3, 116.5, 117.1, 118.7, 120.2, 122.1, 122.7, 123.1, 123.3, 125.5, 126.9, 127.1, 128.0, 139.6, 140.0, 140.2, 149.2, 149.3, 149.6, 171.1, 171.2, 171.3; IR (Nujol): ν = 1594, 1619, 1746 cm^{-1} (C=O); MS (LSIMS); m/z 1324 $[M + H]^+$; elemental analysis calcd (%) for $C_{87}H_{93}N_3O_9$: C 78.91, H 7.02, N 3.17; found C 79.04, H 7.00, N 3.17.

Compound 5b

Due to the insolubilty of this material in all common NMR solvents it proved impossible to fully characterise this material. IR (KBr): ν = 1753 cm^{-1} (C=O); MS (LSIMS); m/z 1904 $[M + H]^+$.

Compound 12a

To a solution of carbazole (1.0 g, 6.0 mmol), in DMF–THF (1 : 2, 25 mL), was added sodium hydride (0.28 g, 12 mmol, 60% in oil) at room temperature. The mixture was stirred for 15 minutes before addition of 1,6-dibromohexane (7.3 g, 30 mmol) and stirred for 10 hours. The reaction was quenched with MeOH (25 mL) and the mixture evaporated to dryness. The residue was partitioned between CH_2Cl_2 (50 mL) and 3 M HCl aq (50 mL). The organic layer was separated and washed with H_2O (60 mL), dried with anhydrous Na_2SO_4, filtered and

the filtrate was evaporated to dryness under reduced pressure, and the residue was subjected to silica gel column chromatography (eluent: hexane–CH_2Cl_2, 1 : 1) to afford **12a** (0.510 g, 26%) as a white microcrystalline powder and **12a.dimer** as a white solid: **12a**: ^{1}H NMR (300 MHz, $CDCl_3$, 21 °C): δ = 1.47–1.38 (m, 4 H), 1.92–1.78 (m, 4 H), 3.36 (t, J = 15.0 Hz, 2 H), 4.32 (t, J = 15.0 Hz, 2 H), 7.25–7.20 (m, 2 H), 7.49–7.38 (m, 4 H), 8.10 (d, J = 9.0 Hz, 2 H); ^{13}C NMR (125 MHz, $CDCl_3$, 31 °C): δ = 26.5, 27.9, 28.8, 32.6, 42.8, 108.6, 118.0, 118.8, 120.4, 122.8, 125.6, 140.4; MS (LSIMS); m/z 331 $[M + H]^+$; elemental analysis calcd (%) for $C_{18}H_{20}NBr$: C 65.45, H 6.06, N 4.24; found C 65.49, H 6.12, N 4.13. **12a.dimer**: ^{1}H NMR (500 MHz, $CDCl_3$, 31 °C): δ = 1.80–1.95 (m, 6 H), 4.20–4.30 (m, 6 H), 7.28–7.30 (m, 8 H), 7.45–7.55 (m, 4 H), 8.12–8.20 (m, 4 H); ^{13}C NMR (125 MHz, $CDCl_3$, 31 °C): δ = 26.8, 42.6, 108.5, 118.9, 120.45, 122.8, 125.7, 140.2; MS (LSIMS): m/z 417 $[M + H]^+$.

The same procedure for **12a** was followed for the synthesis of **12b**, **13a**, **13b** and **13c**. (Quantities used for these N-alkylation reactions are shown in Table 3 of the supplementary material.‡)

Compound 12b. ^{1}H NMR (500 MHz, $CDCl_3$, 31 °C): δ = 1.40–1.24 (m, 8 H), 1.82–1.76 (m, 2 H), 1.89–1.83 (m, 2 H), 3.35 (t, J = 6.8 Hz, 2 H), 4.28 (t, J = 7.2 Hz, 2 H), 7.23 (ddd, J = 7.8, 0.8, 0.8 Hz, 2 H), 7.39 (d, J = 8.1 Hz, 2 H), 7.47 (ddd, J = 7.2, 1.0, 1.0 Hz, 2 H), 8.10 (d, J = 7.4 Hz, 2 H); ^{13}C NMR (125 MHz, $CDCl_3$, 31 °C): δ = 27.1, 27.9, 28.5, 28.8, 29.1, 32.6, 33.8, 42.9, 108.6, 118.7, 120.3, 122.8, 125.5, 140.4; MS (EIMS): m/z 357 $[M]^+$.

Compound 13a. ^{1}H NMR (500 MHz, $CDCl_3$, 31 °C): δ = 2.22 (q, J = 6.9 Hz, 2 H), 2.35 (t, J = 7.2 Hz, 2 H), 3.67 (s, 3 H), 4.39 (t, J = 7.0 Hz, 2 H), 7.2 (ddd, J = 7.8, 0.9, 1.0 Hz, 2 H), 7.43 (d, J = 8.1 Hz, 2 H), 7.49 (ddd, J = 7.1, 1.1, 1.1 Hz, 2 H), 8.12 (d, J = 7.7 Hz, 2 H); ^{13}C NMR (125 MHz, $CDCl_3$, 31 °C): δ = 23.9, 30.8, 41.8, 51.5, 108.5, 118.9, 120.3, 122.8, 125.6, 140.3, 173.2; MS (EIMS): m/z 267 $[M]^+$.

Compound 13b. ^{1}H NMR (500 MHz, $CDCl_3$, 31 °C): δ = 1.45–1.39 (m, 2 H), 1.67 (q, J = 7.4 Hz, 2 H), 1.90 (q, J = 7.3 Hz, 2 H), 2.28 (t, J = 7.4 Hz, 2 H), 3.64 (s, 3 H), 4.30 (t, J = 7.1 Hz, 2 H), 7.26 (ddd, J = 7.7, 0.9, 1.0 Hz, 2 H), 7.40 (d, J = 8.1 Hz, 2 H), 7.49 (ddd, J = 8.1, 1.1, 1.1 Hz, 2 H), 8.12 (d, J = 7.7 Hz, 2 H); ^{13}C NMR (125 MHz, $CDCl_3$, 31 °C): δ = 24.6, 26.7, 28.5, 29.6, 33.7, 34.0, 42.7, 51.3, 108.5, 118.7, 120.3, 122.8, 125.5, 140.3, 173.8; MS (EIMS): m/z 295 $[M]^+$.

Compound 13c. ^{1}H NMR (500 MHz, $CDCl_3$, 31 °C): δ = 1.34 (m, 6 H), 1.61 (q, J = 6.7 Hz, 2 H), 1.87 (q, J = 7.1 Hz, 2 H), 2.28 (t, J = 7.4 Hz, 2 H), 3.67 (s, 3 H), 4.29 (t, J = 7.2 Hz, 2 H) , 7.24 (ddd, J = 7.8, 0.8, 0.7 Hz, 2 H), 7.40 (d, J = 8.1 Hz, 2 H), 7.47 (ddd, J = 8.1, 1.0, 1.0 Hz, 2 H), 8.12 (d, J = 7.74 Hz, 2 H); ^{13}C NMR (125 MHz, $CDCl_3$, 31 °C): δ = 24.7, 27.0, 28.8, 28.9, 29.0, 33.9, 42.9, 51.3, 108.5, 118.6, 120.2, 122.8, 125.5, 140.3, 174.0; MS (ES): m/z 346 $[M + Na]^+$.

Compound 14a

A solution of compound **13a** (0.500 g, 1.87 mmol) in MeOH (100 mL) was heated under reflux and a solution of sodium hydroxide (0.112 g, 2.80 mmol) in H_2O (10 mL) was added under stirring and heating continued for 6 hours. After cooling, the reaction mixture was poured onto crushed ice. The precipitate which formed on acidification with dilute aqueous HCl was then extracted with Et_2O (3 × 50 mL). The combined organic layers were washed with H_2O (5 mL) and brine (5 mL), and dried ($MgSO_4$). Filtration and evaporation of the filtrate gave the crude product which was purified by silica gel column chromatography (eluent: hexane–EtOAc) to yield the acid **14a** as a white solid: ^{1}H NMR (500 MHz, $CDCl_3$, 31 °C): δ = 2.23 (ABq, J = 14.0 Hz, 2 H), 2.43 (t, J = 7.15 Hz, 2 H), 4.40 (t, J = 7.0 Hz, 2 H), 7.26 (br t, J = 7.1 Hz, 2 H), 7.43 (d, J = 8.1 Hz, 2 H), 7.49 (ddd, J = 8.0, 0.8, 0.9 Hz, 2 H), 8.12 (d, J = 7.7 Hz, 2 H), 13.5–9.5 (br envelope, 1 H); ^{13}C NMR (125 MHz, $CDCl_3$, 31 °C): δ = 23.7, 31.0, 41.8, 108.4, 119.0, 120.0, 122.9, 125.7, 140.3, 179.1; MS (EIMS): m/z 253 $[M]^+$; elemental analysis calcd (%) for $C_{16}H_{15}NO_2$: C 75.88, H 5.92, N 5.53; found C 76.23, H 5.97, N 5.53.

Compound 14b. ^{1}H NMR (500 MHz, $CDCl_3$, 31 °C): δ = 1.44 (m, 2 H), 1.68 (q, J = 7.4 Hz, 2 H), 1.90 (q, J = 7.3 Hz, 2 H), 2.32 (t, J = 7.4 Hz, 2 H), 4.30 (t, J = 7.1 Hz, 2 H), 7.24 (ddd, J = 7.8, 1.1, 1.1 Hz, 2 H), 7.39 (d, J = 8.1 Hz, 2 H), 7.47 (ddd, J = 8.1, 1.1, 1.1 Hz, 2 H), 8.1 (d, J = 7.7 Hz, 2 H); ^{13}C NMR (125 MHz, $CDCl_3$, 31 °C): δ = 24.3, 26.6, 28.6, 33.7, 42.7, 108.5, 118.8, 120.3, 122.8, 125.6, 140.3, 179.5; MS (EIMS): m/z 281 $[M]^+$; elemental analysis calcd (%) for $C_{18}H_{19}NO_2$: C 76.88, H 6.76, N 4.98; found C 76.84, H 6.60, N 4.97.

Compound 14c. ^{1}H NMR (500 MHz, $CDCl_3$, 31 °C): δ = 1.38–1.27 (m, 6 H), 1.60–1.54 (m, 2 H), 1.88–1.82 (m, 2 H), 2.28 (t, J = 7.4 Hz, 2 H), 4.27 (t, J = 7.2 Hz, 2 H), 7.23 (ddd, J = 8.5, 0.9, 0.9 Hz, 2 H), 7.38 (d, J = 8.1 Hz, 2 H), 7.45 (ddd, J = 7.1, 1.1, 1.1 Hz, 2 H), 8.08 (d, J = 7.6 Hz, 2 H); ^{13}C NMR (125 MHz, $CDCl_3$, 31 °C): δ = 24.5, 27.1, 28.8, 29.0, 33.7, 43.0, 108.6, 118.7, 120.3, 122.8, 125.5, 140.4, 179.0; MS (EIMS): m/z 309 $[M]^+$; elemental analysis calcd (%) for $C_{20}H_{23}NO_2$: C 77.66, H 7.44, N 4.53; found C 77.59, H 7.53, N 4.46.

Acknowledgements

This research has been supported by the (i) EPSRC (MB), (ii) Leverhulme Trust (MM), (iii) Perkin-Elmer/HEFCE in the UK through the Joint Research Equipment Initiative (JREI).

References

1 (*a*) J. T. Link, S. Raghavan, M. Gallant, S. Danishefsky, T. C. Chou and L. M. Ballas, *J. Am. Chem. Soc.*, 1996, **118**, 2825; (*b*) Y. Yamashita, N. Fujii, C. Murkata, T. Ashiawa, M. Okabe and H. Nakano, *Biochemistry*, 1992, **31**, 12069; (*c*) D. P. Chakraborty, *Prog. Chem. Org. Nat. Prod.*, Vol. 34, ed. W. Heiz, H. Grisebach and G. W. Kirby, Springer, Wien, 1997, p. 299.
2 Y. Zhang, T. Wada and H. Sasabe, *J. Mater. Chem.*, 1998, **8**, 809.
3 The space charge field induced photorefractive effect was first observed in inorganic electro-optic $LiNbO_3$ crystals by A. Ashkin, G. D. Boyd, J. M. Dziedic, R. G. Smith, A. A. Ballman and K. Nassau, *Appl. Phys. Lett.*, 1966, **9**, 72.
4 The first report of a carbazole containing photorefractive material was by Y. Zhang, Y. Cui and P. N. Prasad, *Phys. Rev. B*, 1992, **46**, 9900.
5 *Photorefractive Materials and Their Applications*, ed. P. Günter and J.-P. Huignard, Springer-Verlag, New York, 1988.
6 S. Maruyama, X.-t. Tao, H. Hokari, T. Noh, Y. Zhang, T. Wada, H. Sasabe, T. Watanabe and S. Miyata, *J. Mater. Chem.*, 1999, **9**, 893.
7 Y. Zhang, L. Wang, T. Wada and H. Sasabe, *Chem. Commun.*, 1996, 559.
8 J. C. Scott, L. Th. Pautmeier and W. E. Moerner, *J. Opt. Soc. Am. B*, 1992, **9**, 2059.
9 The first report of an amorphous organic photorefractive material was by S. Ducharme, J. C. Scott, R. J. Twieg and W. E. Moerner, *Phys. Rev. Lett.*, 1991, **66**, 1846.
10 K. Sutter, J. Hulliger and P. Günter, *Solid State Chem.*, 1990, **74**, 867.
11 Y. Zhang, T. Wada, L. Wang and H. Sasabe, *Chem. Mater.*, 1997, **9**, 2798.
12 The carbazole moiety has been introduced into a low molecular

weight calamitic mesogenic structure which diplays a nematic mesophase, see M. Lux and P. Strohriegl, *Makromol. Chem.*, 1987, **188**, 811. Additionally, a report of a polydiacetylene incorporating pendant carbazole moieties has been shown to organise into a self-organised structure, with columnar mesophases from room temperature to 250 °C, see: B. Gallot, A. Cravino, I. Moggio, D. Comoretto, C. Cuniberti, C. Dell'erba and G. Dellepiane, *Liq. Cryst.*, 1999, **26**, 1437.

13 B. Marcher, L. Chapoy and D. H. Christensen, *Macromolecules*, 1988, **21**, 677.

14 M. Manickam, S. Kumar, J. A. Preece and N. Spencer, *Liq. Cryst.*, 2000, **27**, 703.

15 We have chosen the triphenylene mesogenic structure for several reasons: (i) they have pronounced photoconductivity (J. Simmerr, B. Glüsen, W. Paulus, A. Kettner, P. Schumacher, D. Adam, K. H. Etzbach, K. Siemeseyer, J. H. Wendorf, H. Ringsdorf and D. Haarer, *Adv. Mater.*, 1996, **8**, 815), (ii) they have a strong tendency to form columnar mesophases (S. Chandresekhar and S. Kumar, *Science Spectra*, 1997, **8**, 66; M. T. Allen, S. Diele, K. D. M. Harris, T. Hegmann, N. Kumari, B. M. Kariuki, D. Lose, J. A. Preece and C. Tschierske, *Liq. Cryst.*, 2000, **27**, 689), and it is well recognised that the supramolecular structure of disc-shaped molecules, in general, is well suited for the one dimensional charge migration (see D. Markovitski, S. Marguet, L. K. Gallos, H. Sigal, P. Millie, P. Argyrakis, H. Ringsdorf and S. Kumar, *Chem. Phys. Lett.*, 1999, **306**, 163) and one dimensional chain migration (see N. Boden, R. C. Borner, R. J. Bushby and J. Clements, *J. Am. Chem. Soc.*, 1994, **116**, 10807; V. S. K. Balagurusamy, S. Krishna Prasad, S. Chandrasekhar, S. Kumar, M. Manickam and C. V. Yelamaggad, *Pramana*, 1999, **53**, 3) as well as ferroelectrical properties (see H. Bock and W. Helfrich, *Liq. Cryst.*, 1995, **18**, 387), optoelectrical switching behaviour (C. Y. Lin, H. L. Pan, M. A. Fox and A. J. Bard, *Science*, 1993, **261**, 897), and photovoltaic behaviour (B. A. Greg, M. A. Foc and A. J. Bard, *J. Phys. Chem.*, 1990, **94**, 1586), and (iii) doping with TNF can induce liquid crystalline behaviour in many triphenylene materials that initially do not show mesophase properties, W. Kranig, C. Boefield and H. W. Spiess, *Liq. Cryst.*, 1990, **8**, 375; H. Bengs, O. Karthaus, H. Ringsdorf, C. Baehr, M. Ebert and J. H. Wendorf, *Liq. Cryst.*, 1999, **10**, 161.

16 (*a*) D. Markovitski, N. Pfeffen, F. Charra, J.-M. Nunzi, H. Bengs and H. Ringsdorf, *J. Chem. Soc., Faraday Trans.*, 1993, **89**, 37; (*b*) N. Boden, R. J. Bushby and J. F. Hubbard, *Mol. Cryst Liq. Cryst.*, 1997, **304**, 195; (*c*) A. Stracke, J. H. Wendorf, D. Janietz and S. Mahlstedt, *Adv. Mater.*, 1999, **11**, 667; (*d*) K. Praefcke and D. Singer, *Handbook of Liquid Crystals*, ed D. Demus, G. W. Gray, H. W. Spiess and V. Vill, vol 2B, 1998, pp. 943–967.

17 S. Kumar and M. Manickam, *Synthesis*, 1998, 1119.

18 F. C. Krebs, N. E. Schmidt, W. Batsberg and K. Bechgaard, *Synthesis*, 1997, 1285.

19 (*a*) H. Bengs, O. Karthaus, H. Ringsdorf, C. Baehr, M. Ebert and J. N. Wendorff, *Liq. Cryst.*, 1991, **10**, 161; (*b*) N. Boden, R. C. Burner, R. J. Bushby, A. N. Cammidge and M. V. Jesudason, *Liq. Cryst.*, 1993, **15**, 851.

20 (*a*) Y. Zhang, T. Wada and H. Sasabe, *Chem. Commun.*, 1996, 621; (*b*) J. W. Taylor, C. P. Sloan, D. A. Holden, G. J. Kovacs and R. O. Loutfy, *Can. J. Chem.*, 1989, **67**, 2142.

21 H. Bengs, M. Ebert, O. Karthaus, B. Kohne, K. Praefcke, H. Ringsdorf, J. H. Wendorf and R. Wusterfield, *Adv. Mater.*, 1990, **2**, 141.

22 S. Kumar, M. Manickam, S. K. Varshney, D. S. Shankar Rao and S. K. Prasad, *J. Mater. Chem.*, 2000, **10**, 2483.

23 M. Belloni, M. Manickam, P. R. Ashton, B. Kariuki, J. A. Preece, N. Spencer and J. Wilkie, *Mol. Cryst. Liq. Cryst*, in the press.

24 (*a*) D. Singer, A. Liebman, K. Praefcke and J. H. Wendorf, *Liq. Cryst.*, 1993, **14**, 785; (*b*) H. Ringsdorf, R. Wusterfeld, E. Zerta, M. Ebert and J. H. Wendorf, *Angew. Chem., Int. Ed. Engl.*, 1989, **28**, 914.

25 (*a*) S. Kumar, D. S. Shankar Rao and S. Krishna Prasad, *J. Mater. Chem.*, 1999, **9**, 2751; (*b*) S. Kumar, M. Manickam, V. S. K. Balagurasamy and H. Schonherr, *Liq. Cryst.*, 1999, **26**, 1455.